Available online at www.sciencedirect.com
SCIENCE DIRECT®
Journal of Magnetic Resonance 168 (2004) 327–335
JMR Journal of Magnetic Resonance
www.elsevier.com/locate/jmr

Uniform-sign cross-peak double-quantum-filtered correlation spectroscopy

Leonard J. Mueller,[a,*] Douglas W. Elliott,[a] Garett M. Leskowitz,[a] Jochem Struppe,[b] Ryan A. Olsen,[a] Kee-Chan Kim,[a] and Christopher A. Reed[a]

[a] *Department of Chemistry, University of California, Riverside, CA 92521, USA*
[b] *Bruker BioSpin Corporation, Billerica, MA 01821, USA*

Received 2 October 2003; revised 18 March 2004
Available online 22 April 2004

Abstract

We detail the uniform-sign cross-peak double-quantum-filtered correlation spectroscopy (UC2QF COSY) experiment, a new through-bond correlation method for disordered solids. This experiment is a refocused version of the popular double-quantum-filtered correlation spectroscopy experiment in liquids. Its key feature is that it provides in-phase and doubly absorptive line shapes, which renders it robust for chemical shift correlation in solids. Both theory and experiment point to distinct advantages of this protocol, which are illustrated by several experiments under challenging conditions, including fast magic-angle spinning (30 kHz), anisotropic molecular motion, and ^{13}C correlation spectroscopy at the natural abundance isotope level.

Keywords: UC2QF COSY; Solid-state NMR; Scalar-coupling-driven correlation; Through-bond correlation; Natural abundance ^{13}C correlation

1. Introduction

Solid state NMR spectra of disordered solids are typically acquired under magic-angle-spinning conditions in which anisotropic interactions, such as chemical shift anisotropy and low-γ homonuclear and heteronuclear dipolar couplings, are effectively averaged to zero. Combined with high-power proton decoupling, spectral line widths are often reduced from many tens of kilohertz in static solids to hundreds of hertz or less. Even with such improved resolution, homonuclear scalar couplings are rarely resolved between typical observe nuclei such as ^{13}C, ^{31}P, and ^{29}Si. Still, scalar couplings are present in the solid state and provide a mechanism for magnetization transfer and correlation spectroscopy. There has recently been significant interest in scalar-coupling-driven correlation in solids as a tool for establishing through-bond connectivity, for facilitating spectral assignment, and as a complementary method to dipolar-driven correlation spectroscopy [1–12]. Indeed, scalar coupling-driven correlation in solids complements the more popular dipolar-driven methods in two ways. First, as the dipolar coupling provides distance constraints and the scalar coupling provides covalent connectivity, the combination of the two allows one to delineate through-bond and through-space connectivity, a critical step for establishing structure. Second, unlike dipolar interactions, which can average to zero under molecular motion even in the solid state, scalar couplings are relatively insensitive to global molecular dynamics and can provide for correlation and spectral assignment in situations where dipolar-driven experiments fail.

Two general approaches to scalar-coupling-driven correlation in solids have developed. One method, the analogue of the TOCSY experiment in liquid-state NMR, [13] makes use of rotor-synchronized radio-frequency nutation fields to produce the strong scalar-coupling or isotropic-mixing Hamiltonian, $JI \cdot S$ [3,6,7]. Efficient correlation can be achieved in these experiments even in the absence of resolved couplings. However, RF power requirements ultimately limit the practical MAS rates for which many of these experiments can be performed. The difficulty is that the

* Corresponding author. Fax: 1-909-7874713.
E-mail address: Leonard.Mueller@ucr.edu (L.J. Mueller).

1090-7807/$ - see front matter © 2004 Elsevier Inc. All rights reserved.
doi:10.1016/j.jmr.2004.03.017

required nutation frequency is a multiple of the MAS rate (typically 3.5–7) and the proton decoupling field must be at least a factor of three greater than this to maintain efficient decoupling [14,15].

A second approach to scalar-coupling-driven correlation in solids is analogous to COSY-based experiments in liquid-state NMR, with coherences transferred via the weak scalar-coupling interaction, JI_zS_z. A number of techniques in liquid-state NMR have been developed to effect correlation under the weak scalar-coupling Hamiltonian [16], and in principle these experiments could also be applied to solids. Unfortunately, the two most important examples of weak scalar-coupling-driven correlation in liquids, the double-quantum-filtered COSY (2QF COSY) [17,18] and the INADEQUATE experiment [19], are not optimum for use in solids since they produce anti-phase line shapes that lead to cross-peak intensity cancellation when the coupling is unresolved. The refocused-INADEQUATE experiment was originally developed in liquid-state NMR to combat this problem. By introducing refocusing periods into the pulse sequence, in-phase line shapes are observed. Emsley [4] has shown that the refocused INADEQUATE is also effective in solids. Since relaxation during echo periods is typically much slower than during direct observation, these sequences can have good transfer efficiency. Meier [5] has shown similar results with the related INADEQUATE-CR.

Recently, we introduced the uniform-sign cross-peak double-quantum filtered correlation spectroscopy (UC2QF COSY) experiment as an effective through-bond correlation spectroscopy for disordered solids [11]. This refocused version of the 2QF COSY also provides in-phase cross-peaks, but does so while maintaining the 2QF COSY's single quantum–single quantum chemical shift correlation framework and avoiding the faster relaxation present in the double-quantum domain of the refocused INADEQUATE. As with the refocused INADEQUATE, magnetization is transferred through the scalar coupling during chemical shift refocusing periods where the effective resolution is much higher and the transfer more efficient than during free evolution. In this way, the UC2QF COSY is robust for solids and shows excellent correlation even in the presence of unresolved scalar couplings. In this paper, we detail the UC2QF COSY and quantify the sensitivity advantage of its refocusing strategy relative to the original 2QF COSY for applications in solids. A number of practical considerations and experiments are discussed. These illustrate the UC2QF COSY's robust performance under fast MAS (30 kHz) and in the presence of anisotropic molecular motion. We also point out the excellent sensitivity that can be obtained with the UC2QF COSY, which is high enough for ^{13}C correlation spectroscopy at the natural abundance isotope level.

2. The UC2QF COSY

The 2QF COSY experiment [17,18] is one of the most important experiments in liquid-state NMR for determining through-bond connectivity and is often the first step in establishing the spectral assignment in liquid state NMR investigations. A central characteristic of this scalar-coupling-driven experiment is the purely absorptive character of both the diagonal and cross-peaks, which provides considerably better resolution than is possible with earlier versions of the COSY experiment [20]. As noted above, the original 2QF COSY experiment (Fig. 1A) is far less useful in solid-state applications because its cross-peaks have an anti-phase relationship (Fig. 1B) in which the doublet components (split in frequency by the scalar coupling) have opposite sign. When the spectral line widths are larger than the scalar couplings, significant intensity cancellation occurs, and the through-bond correlation is difficult to ascertain. To provide a robust 2QF COSY experiment for solids it is necessary to transform the cross-peaks from anti-phase to in-phase, in which the doublet components have a uniform sign. This transformation is accomplished through standard "refocusing" pulse sequence elements that we append to the original pulse sequence to give a novel variant of the 2QF COSY (Fig. 1C). The desired coherence pathway can be achieved through phase-cycling [21], and this leads to a correlation spectroscopy with diagonal and cross-peaks in pure absorption mode and in-phase, that is, with uniform algebraic sign (Fig. 1D). We call this refocused variant the uniform-sign cross-peak (UC) 2QF COSY. Three versions of the UC2QF COSY pulse sequence and coherence level diagrams are shown in Fig. 2.

Analysis of the UC2QF COSY is straightforward. The key to creating in-phase, doubly absorptive cross-peaks is a mixing period that converts I_x magnetization into the sum $\frac{1}{2}(I_x + S_x)$. This transformation is accomplished in several steps. First, I_x evolves into anti-phase magnetization under the scalar-coupling interaction, JI_zS_z:

$$I_x \xrightarrow{\tau-\pi-\tau} 2I_yS_z.$$

This transformation takes place over a time interval $2\tau = 1/(2J)$, during which chemical shift is refocused with π pulses on both I and S spins. The relatively long refocusing period ($\sim$10 ms for typical 50 Hz $^1J_{CC}$ couplings) may seem incompatible with solid-state NMR, where one would expect significant intensity loss due to relaxation during this time. However, the relaxation rate under echo sequences, $1/T_2'$, is governed primarily by the homogeneous line width and is significantly slower than the relaxation rate of the directly observed signal, $1/T_2^*$, which is governed by the inhomogeneous line width [22]. Such refocusing periods can in fact be very useful in solid-state studies [4,5].

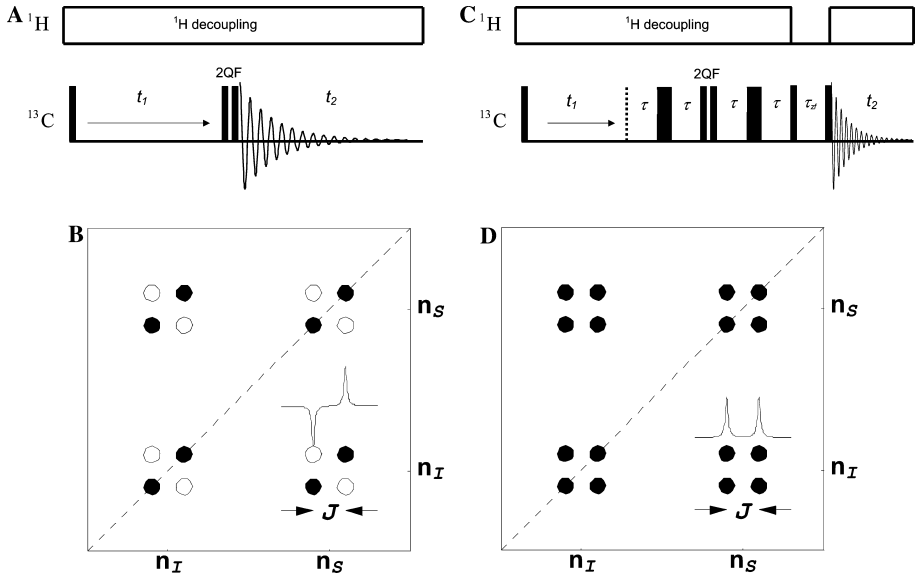

Fig. 1. Chemical shift correlation spectroscopy using the 2QF COSY (A and B) and the UC2QF COSY (C and D). Thin vertical lines in the pulse sequences indicate $\pi/2$ pulses, thick vertical lines indicate π pulses, and the double-quantum-filtering pulse pair [21] is labeled 2QF. The 2QF COSY gives rise to 2D correlation spectra in which the diagonal and cross-peaks are anti-phase. The UC2QF COSY experiment appends two τ–π–τ refocusing elements about the double-quantum filter and a final z-filter (zf) to produce a correlation spectrum with in-phase cross-peaks. The refocusing delay τ is set to an integral number of rotor periods to rigorously refocus the chemical shift interaction, and maximum signal intensity is obtained in 2-spin systems for $\tau = 1/4J_{IS}$. Although shown with a $\pi/2$ preparation pulse, cross-polarization [36] is appropriate in many cases. Pure phase spectra can be obtained using the method of States [37].

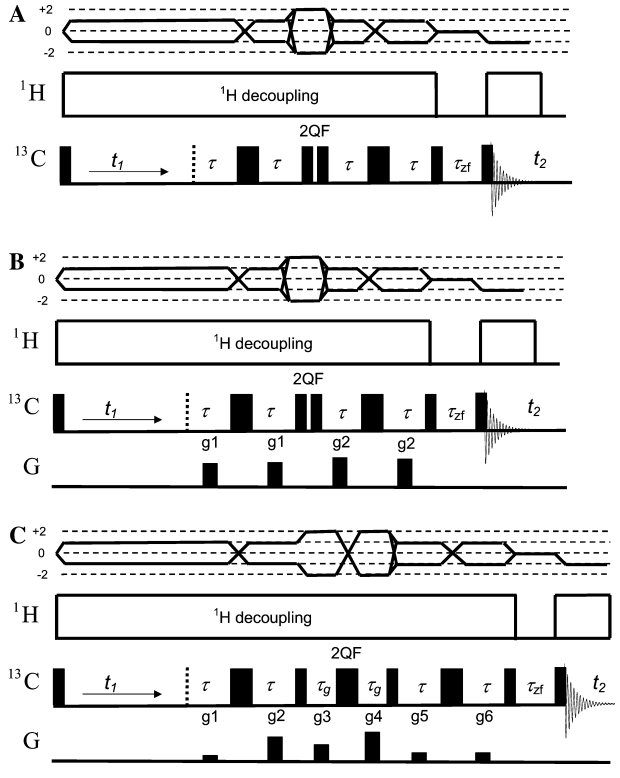

Fig. 2. Three variations of the UC2QF COSY. Versions (A) and (B) are identical except for the use of gradient π pulse selection in (B). In (C), the full coherence pathway is selected using gradients following the 2QF COSY scheme of Keeler [27]. Possible relative values of the gradients in (C) include $g_1 = 5$, $g_2 = 27$, $g_3 = 15$, $g_4 = 26$, $g_5 = 8$, and $g_6 = 8$. The refocusing delay τ is set as described in Fig. 1.

In the second step, anti-phase magnetization $2I_yS_z$ is transformed into double quantum coherence with $\pi/2$ pulses on both I and S spins and then selected with a double quantum filter (2QF):

$$2I_yS_z \xrightarrow{\frac{\pi}{2}(I_y+S_y)} 2I_yS_x \xrightarrow{2\mathrm{QF}} (I_yS_x + I_xS_y).$$

The double quantum filter removes unwanted residual linear spin operators and also the zero-quantum component, $I_xS_y - I_yS_x$. Removal of the latter is critical—if zero-quantum coherence is not destroyed, no net magnetization is transferred to the S spin. Next, the double-quantum coherence is converted back to anti-phase magnetization, now equally distributed over the I and S spins, with $\pi/2$ pulses. Another τ–π–τ evolution interval follows, during which the anti-phase magnetization evolves into the sum $\frac{1}{2}(I_x + S_x)$. This sum is uniquely selected by the final z-filter (zf), [23] which suppresses unwanted residual terms:

$$(I_yS_x + I_xS_y) \xrightarrow{\frac{\pi}{2}(I_y+S_y)} (I_yS_z + I_zS_y) \xrightarrow{\tau-\pi-\tau} \tfrac{1}{2}(I_x + S_x) \xrightarrow{\mathrm{zf}} \tfrac{1}{2}(I_x + S_x).$$

The in-phase cross-peaks effected by the transformation of I_x magnetization into the sum $\frac{1}{2}(I_x + S_x)$ are purchased at the cost of additional relaxation during a total delay of $4\tau = 1/J$. If the attenuation of the signal due to this relaxation is small enough not to offset the advantage gained by converting anti-phase cross-peaks to in-phase peaks, then there is a net gain in efficiency. We can quantify the efficiency of the refocusing strategy relative to the original 2QF COSY by comparing signal

energies, which we carry out explicitly for a two-spin system. In the UC2QF COSY the two-dimensional signal for both the diagonal and cross-peaks is

$$S_{\mathrm{UC2QF}}(t_1,t_2) = f(J,T_2')\mathrm{e}^{-(t_1+t_2)/T_2^*}\cos(\pi J t_1)\cos(\pi J t_2),$$

where the cosine modulation in both t_1 and t_2 is characteristic of the in-phase multiplet structure and where

$$f(J,T_2') = \mathrm{e}^{-4\tau/T_2'}\sin^2(2\pi J\tau)$$

is the intensity attenuation introduced by the two τ–π–τ evolution intervals. $f(J,T_2')$ achieves its maximum value at $\tau_{\max} = \frac{1}{2\pi J}\tan^{-1}(\pi J T_2')$, giving

$$f(J,T_2')_{\max} = \frac{(\pi J T_2')^2}{1+(\pi J T_2')^2}\exp\left[-\frac{2}{\pi J T_2'}\tan^{-1}(\pi J T_2')\right].$$

In the limit of long T_2', $\tau_{\max}$ is $1/4J$ and $f(J,T_2')_{\max} = 1$. For shorter values of T_2', the maximum occurs at $\tau < 1/4J$, and $f_{\max}$ is less than 1.

In the original 2QF COSY experiment, the two-dimensional signals for the diagonal and cross-peaks are anti-phase with respect to both the direct and indirect frequency domains. This corresponds to a time-domain signal that is sine-modulated in both t_1 and t_2:

$$S_{\mathrm{2QF}}(t_1,t_2) = \mathrm{e}^{-(t_1+t_2)/T_2^*}\sin(\pi J t_1)\sin(\pi J t_2).$$

The ratio of the signal energies,

$$R = \int \mathrm{d}t_1\mathrm{d}t_2\ S_{\mathrm{UC2QF}}(t_1,t_2)^2 \Big/ \int \mathrm{d}t_1\mathrm{d}t_2\ S_{\mathrm{2QF}}(t_1,t_2)^2$$

quantifies the relative effects of the observed line width (governed by the inhomogeneous relaxation time T_2^*), the echo line width (determined by T_2'), and the size of the scalar coupling J. When R is greater than one, the refocused 2QF COSY is superior to the original 2QF COSY in terms of the signal energy and is the preferred experiment. When R is less than one, the original 2QF COSY is preferred.

Integrating the signals and substituting in the maximum value of $f(J,T_2')$, we find

$$R = \left[\frac{2+(\pi J T_2^*)^2}{1+(\pi J T_2')^2}\right]^2\left(\frac{T_2'}{T_2^*}\right)^4\exp\left[-\frac{4}{\pi J T_2'}\tan^{-1}(\pi J T_2')\right],$$

which can be written in terms of the dimensionless variables $j = \pi J T_2^*$, the scalar coupling in units of the observed line width, and $r = T_2'/T_2^* > 1$, the ratio of the echo to direct-observe decay times:

$$R = \left(\frac{2+j^2}{1+j^2r^2}\right)^2 r^4\exp\left[-\frac{4}{jr}\tan^{-1}(jr)\right].$$

Fig. 3 shows contours of R as a function of j and r. Three distinct regions are evident. The first is the region $r < 2$, which is the case when $T_2' < 2T_2^*$. Here, as one would expect for echo relaxation times comparable to the direct-observe T_2^*, the original 2QF COSY is the preferred experiment. When $T_2' > 2T_2^*$ and the scalar couplings are unresolved ($j < 1$), the UC2QF COSY has a significant sensitivity advantage. In the regime where $0.5 < R < 2$ the two experiments are of approximately the same effectiveness. We note that the only regime in which the UC2QF COSY is not a practical alternative to the 2QF COSY is when the ratio of T_2's is less than two, a situation that is typically not the case in solid-state NMR. In order to use the UC2QF COSY effectively, however, one requires an estimate of $\tau_{\max}$. In most cases this can be empirically optimized by maximizing the signal for $t_1 = 0$.

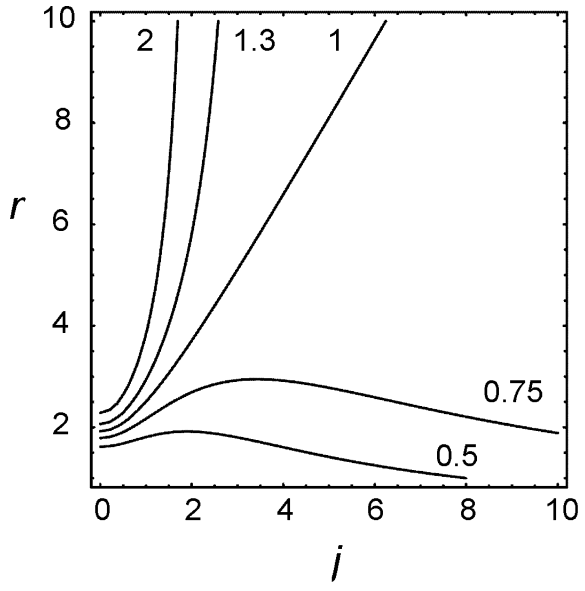

Fig. 3. The energy ratio, R, of the UC2QF COSY to the 2QF COSY as a function of the reduced scalar-coupling constant, $j = \pi J T_2^*$ and the ratio of the echo to direct-observe decay times $r = T_2'/T_2^*$. When R is greater than one, the UC2QF COSY is superior to the original 2QF COSY in terms of the signal energy and is the preferred experiment. When R is less than one, the original 2QF COSY is preferred.

3. Results and discussion

Fig. 4 shows the ^{13}C UC2QF COSY spectrum of U–^{13}C, ^{15}Nglycine (diluted to 10% in natural abundance isotopomers). For this system, $^1J_{\mathrm{CC}} \approx 50$ Hz and the choice of $\tau = 1/4J_{\mathrm{CC}} = 5$ ms gives optimal transfer efficiency, with 45% of the magnetization beginning on ^{13}C contributing to the measured signal. The efficiency of the UC2QF COSY depends strongly on the proton decoupling and continues to improve even after the observed line width has reached a minimum. We find good results under both TPPM [24] and SPINAL-64 [25] heteronuclear proton decoupling schemes, which are also optimized by maximizing the signal for $t_1 = 0$.

Several practical aspects of the UC2QF COSY should be noted. First, in order to rigorously implement the coherence pathways in Fig. 2, complete phase cycling of the pulses is essential. Table 1 shows a strict

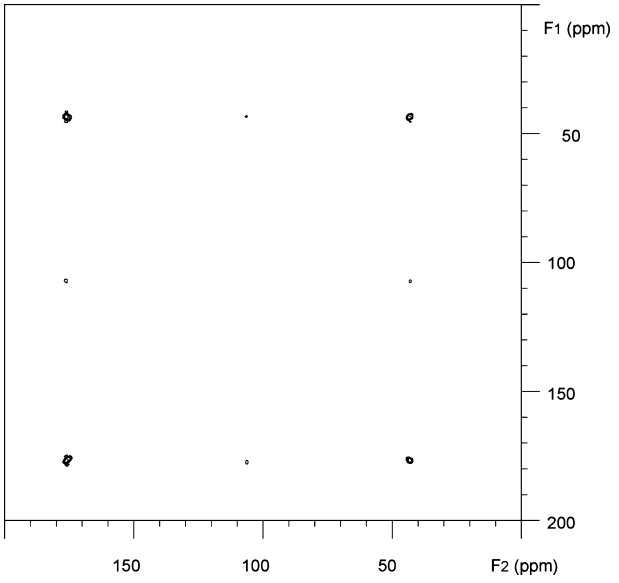

Fig. 4. The ^{13}C UC2QF COSY of U–^{13}C, ^{15}Nglycine (diluted to 10% in unlabeled glycine). Data were acquired on a 9.4 T Bruker DSX spectrometer (^{1}H frequency 400.13 MHz) equipped with a double-resonance 4 mm MAS probe spinning at 5 kHz. The pulse sequence from Fig. 2B was used with the preparatory pulse replaced by cross-polarization from protons. Fifty kilohertz ^{13}C pulses were used throughout, along with 80 kHz TPPM ^{1}H decoupling. The hybrid gradient π selection and shortened phase cycle were used (Fig. 2B). Five hundred and twelve points were acquired with a spectral width of 18 kHz in t_1 and 1024 points were acquired in t_2 with a spectral width of 25 kHz.

Table 1
Complete phase cycling for the UC2QF COSY (Fig. 2A)

Phase	Cycle
ϕ_1	1, 2, 3, 0
ϕ_2	0, 1, 2, 3, 1, 2, 3, 0, 2, 3, 0, 1, 3, 0, 1, 2
ϕ_3	1, 2, 3, 0
ϕ_4	0
ϕ_5	1, 1, 1, 1, 1, 1, 1, 1, 1, 1, 1, 1, 1, 1, 1, 1, 2, 2, 2, 2, 2, 2, 2, 2, 2, 2, 2, 2, 2, 2, 2, 2, 3, 3, 3, 3, 3, 3, 3, 3, 3, 3, 3, 3, 3, 3, 0, 0, 0, 0, 0, 0, 0, 0, 0, 0, 0, 0, 0, 0, 0, 0
ϕ_6	0
ϕ_7	2
ϕ_{rec}	0, 2, 0, 2, 2, 0, 2, 0, 0, 2, 0, 2, 2, 0, 2, 0, 2, 0, 2, 0, 0, 2, 0, 2, 2, 0, 2, 0, 0, 2, 0, 2

The pulse phases are sequentially numbered from the left on the ^{13}C channel. The first three pulses are phase cycled together for double quantum excitation, and the two π pulses (highlighted in gray) are independently phase cycled for a coherence order change of ±2. In this table the phase of the RF is given as integer multiples of 90° (i.e., 0 = "x", 1 = "y", 2 = "$-x$", and 3 = "−y") and the list repeats once the end of the line has been reached. When gradients are incorporated for π selection, only the first four steps of the phase cycle are used.

implementation. This can be time-consuming, and when abundant signal-to-noise renders large numbers of scans per t_1 point unnecessary, gradient-enhanced versions of the experiment are an attractive alternative [26]. Gradient selection can be used in conjunction with partial phase cycling for the double-quantum filter or for selection of the entire coherence pathway. For example, gradient selection of the π pulses in Fig. 2B shortens the phase cycle by a factor of 16, and phase cycling is then only used for the double-quantum filter. Full coherence pathway selection using the version of the sequence shown in Fig. 2C is also possible. This scheme, which follows that used in the gradient 2QF COSY [27], still allows for pure phase acquisition, but suffers a factor of two decrease in signal intensity. The hybrid π pulse gradient selection and shortened phase cycle method, however, does not suffer from reduced signal intensity.

Another important consideration is the z-filter element. In general, this period should be kept as short as possible to minimize spin diffusion. In certain cases, such as in compounds having carbons with no attached protons, longer dephasing times are necessary, particularly at faster spinning speeds. Here, z-axis gradients can again be useful, allowing for the selection of magnetization components during proton decoupling, which suppresses spin diffusion.

The choice of τ is straightforward in two-spin systems. For multi-spin systems, however, the optimum value of τ depends on the number of spins to which a given nucleus is coupled, a feature that is similar to the well-known spectral editing features of experiments such as INEPT [28] and DEPT [29]. Table 2 lists the diagonal and cross-peak intensities as a function of the refocusing interval for $IS_1 - IS_4$ spin systems. We note that in the two-spin system of glycine (Fig. 4), we do observe the expected equal intensity for diagonal and cross-peaks. For a uniformly labeled organic solid, no single choice for τ maximizes cross-peak intensities for all spin systems that might be observed. In a molecule with varying types of spin systems, a reasonable choice for τ is $1/16J - 1/8J$, which has acceptable cross-peak intensities. Fig. 5 shows the UC2QF COSY spectrum of U–^{13}C, ^{15}Ntyrosine·HCl, which has IS, IS_2, and IS_3 spin systems present. This experiment was performed while spinning at 30 kHz. Many dipolar-driven nutation-based experiments have stringent RF matching conditions and also large proton-decoupling requirements that together bring down the transfer efficiency at higher MAS rates. The UC2QF COSY experiment, however, appears to be fairly robust with respect to MAS, and we see no theoretical incompatibility with even higher MAS rates. Recently, Meier [9,10] introduced an adiabatic-pulse version of the TOBSY experiment that also shows excellent correlation spectroscopy at 30 kHz.

While multiple spin systems complicate the setup of the UC2QF COSY with isotopically enriched samples, an important contribution of this work is toward two-dimensional ^{13}C correlation spectroscopy at the natural abundance isotope level. The challenge of natural-abundance ^{13}C spectroscopy is the loss in signal intensity due to the 1% isotope concentration of the spins.

Table 2
Diagonal and cross-peak intensities for the UC2QF COSY as a function of the refocusing period τ in multispin systems

Spin system	Diagonal (spin I)	Cross-peak (from I to S)
IS	$\frac{1}{2}\sin^2(2\pi J\tau)$	$\frac{1}{2}\sin^2(2\pi J\tau)$
IS_2	$\frac{1}{2}\sin^2(2\pi J\tau)[3\cos^2(2\pi J\tau)-1]$	$\frac{1}{2}\cos(2\pi J\tau)\sin^2(2\pi J\tau)$
IS_3	$\frac{1}{2}\sin^2(2\pi J\tau)[6\cos^2(2\pi J\tau)-3]\cos^2(2\pi J\tau)$	$\frac{1}{2}\cos^2(2\pi J\tau)\sin^2(2\pi J\tau)$
IS_4	$\frac{1}{2}\sin^2(2\pi J\tau)[10\cos^2(2\pi J\tau)-6]\cos^4(2\pi J\tau)$	$\frac{1}{2}\cos^3(2\pi J\tau)\sin^2(2\pi J\tau)$

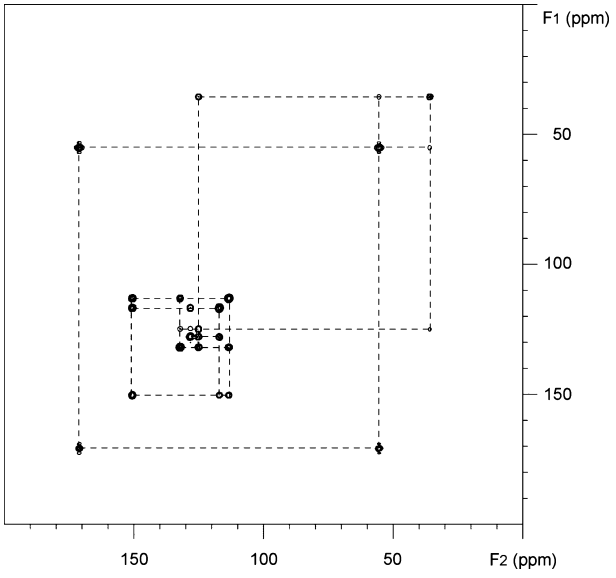

Fig. 5. The ^{13}C UC2QF COSY of U–^{13}C, ^{15}Ntyrosine (diluted to 50% in unlabeled tyrosine). Data were acquired on a 9.4 T Bruker DSX spectrometer (^{1}H frequency 400.13 MHz) equipped with a double-resonance 2.5 mm MAS probe spinning at 30 kHz. The pulse sequence from Fig. 2A was used with the preparatory pulse replaced by cross-polarization from protons. 50 kHz ^{13}C pulses were used throughout, along with 80 kHz TPPM ^{1}H decoupling. The full phase cycle of Table 1 was used. Two hundred and fifty six points were acquired with a spectral width of 25 kHz in t_1 and 1024 points were acquired in t_2 with a spectral width of 25 kHz.

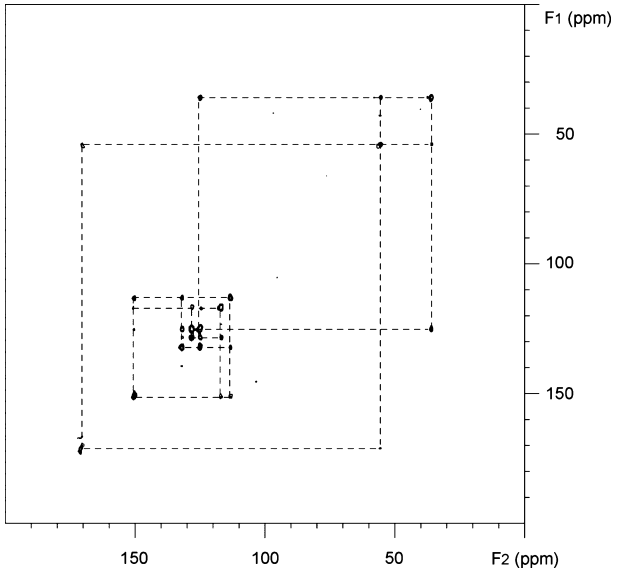

Fig. 6. The ^{13}C UC2QF COSY of unlabeled tyrosine. Data were acquired on an 11.7 T Bruker DSX spectrometer (^{1}H frequency 500 MHz) equipped with a double resonance 4 mm MAS probe spinning at 12 kHz. The pulse sequence from Fig. 2A was used with the preparatory pulse replaced by cross-polarization from protons. Fifty kilohertz ^{13}C pulses were used throughout, along with 100 kHz TPPM ^{1}H decoupling. The full phase cycle of Table 1 was used. Two hundred and fifty six points were acquired with a spectral width of 20 kHz in t_1 and 1024 points were acquired in t_2 with a spectral width of 20 kHz.

This loss is particularly acute for correlation spectroscopy, which relies on the presence of pairs of spin-active nuclei, decreasing the sensitivity of natural-abundance correlation spectroscopy by four orders of magnitude compared to correlation experiments on uniformly labeled materials.

Fig. 6 shows the UC2QF COSY applied to natural abundance correlation in tyrosine·HCl. The complications associated with multiple spin systems are alleviated as the isotope dilution reduces each correlation to a single spin pair and the choice of $\tau = 1/4J$ is optimum. In general, we find that excellent correlation spectroscopy can be performed on smaller molecules ($\sim$10 unique sites) in less than 24 h on a 500 MHz spectrometer with 80 mg of sample. There are far fewer examples of natural abundance ^{13}C correlation experiments reported in solids than in liquids, particularly on molecules with more than a dozen carbon sites [30–34]. Recently, we have shown that ^{13}C natural-abundance correlation in solids can be extended to molecules of moderate size by using the UC2QF COSY to assign the 54 peaks in the solid-state NMR spectrum of microcrystalline vitamin-D_3 [12]. In this case, comparison between the assigned peaks and ab initio calculations of the chemical shifts based on the crystal coordinates permits a refinement of the average structure in dynamic regions reported as disordered in the crystal structure. Even at natural abundance isotope concentrations, where correlation spectroscopy is most challenging, the UC2QF COSY continues to perform well, in part because the relatively low overall power delivered to the ^{13}C channel allows the spectrometer to remain stable during the longer signal averaging periods necessary to increase the signal-to-noise ratio. The acquisition time required to achieve a given signal-to-noise ratio for natural abundance correlation can quickly grow to several days or even weeks and depends critically on the molecular weight and the line width.

A particular advantage of scalar-coupling-driven correlation experiments in general is that, by virtue of the non-zero isotropic component of the scalar coupling, the experiments are insensitive to global molecular motion. This is especially important in the characterization of species such as HC_{60}^{+}, where molecular motion averages dipolar couplings and renders through-space correlation methods ineffective. An important structural question related to HC_{60}^{+} is how the cationic site is disposed relative to the sp^3 hybridized site of protonation. The single-excitation-pulse, 1D ^{13}C spectrum exhibits distinct peaks at the expected frequencies for an sp^3 site and an sp^2 cationic site, in addition to multiple inequivalent sp^2 hybridized carbons. Our attempts to make use of ^{13}C–^{13}C dipolar-driven correlation spectroscopy to determine spatial connectivity, however, failed in this case due to anisotropic molecular motion that severely attenuated the ^{13}C–^{13}C dipolar interactions. Although cross-polarization under the larger ^{1}H–^{13}C heteronuclear dipolar coupling allowed us to confirm the attached proton at the sp^3 site, [35] longer range ^{1}H-^{13}C cross-polarization dynamics were skewed by anisotropic rotational motion under which only the projection of the dipolar couplings along the anisotropic rotation axis survived.

The UC2QF COSY provides a direct and accurate characterization of the through-bond connectivity in HC_{60}^{+} (Fig. 7) [11]. The key spectral feature, the cross-peak between the protonated sp^3 hybridized carbon site at 56 ppm and the sp^2 hybridized cationic site at 182 ppm, indicates that these sites are directly bonded. As the sp^3 and $sp^2(+)$ hybridized sites show only two cross-peaks each, their bond must lie along a molecular plane of symmetry and form the connection of two six-membered rings as shown in the inset. Note that even in the severely overlapped sp^2 region (Fig. 7B), which has 30 nearly degenerate carbons, the in-phase cross-peaks permit an interpretation of connectivity. In contrast, the anti-phase line shape of the original 2QF COSY leads to destructive interference between overlapped resonances, and our best attempts to implement the 2QF COSY showed no cross-peaks either between the $sp^2(+)$ and sp^3 carbons or within the sp^2 region.

Although many of the advantages of the UC2QF COSY are shared with the refocused INADEQUATE and the strong scalar-coupling-driven sequences, there are distinctions between them. For example, both the refocused INADEQUATE and UC2QF COSY focus on the large one-bond $^{1}J_{CC}$ and do not pass relayed coherence transfers. The strong scalar-coupling sequences, however, do show extended cross-peaks throughout the entire coupling network. But, as already noted, these sequences can require relatively high RF powers. Important differences also exist between the refocused INADEQUATE and the UC2QF COSY. Since the refocused INADEQUATE has no diagonal peaks in its double quantum–single quantum correlation map, there may be advantages to its use for assigning congested spectra. However, as the double quantum coherence in t_1 for the refocused INADEQUATE decays at approximately twice the rate of the single quantum coherence in t_1 for the UC2QF COSY, there are potential sensitivity

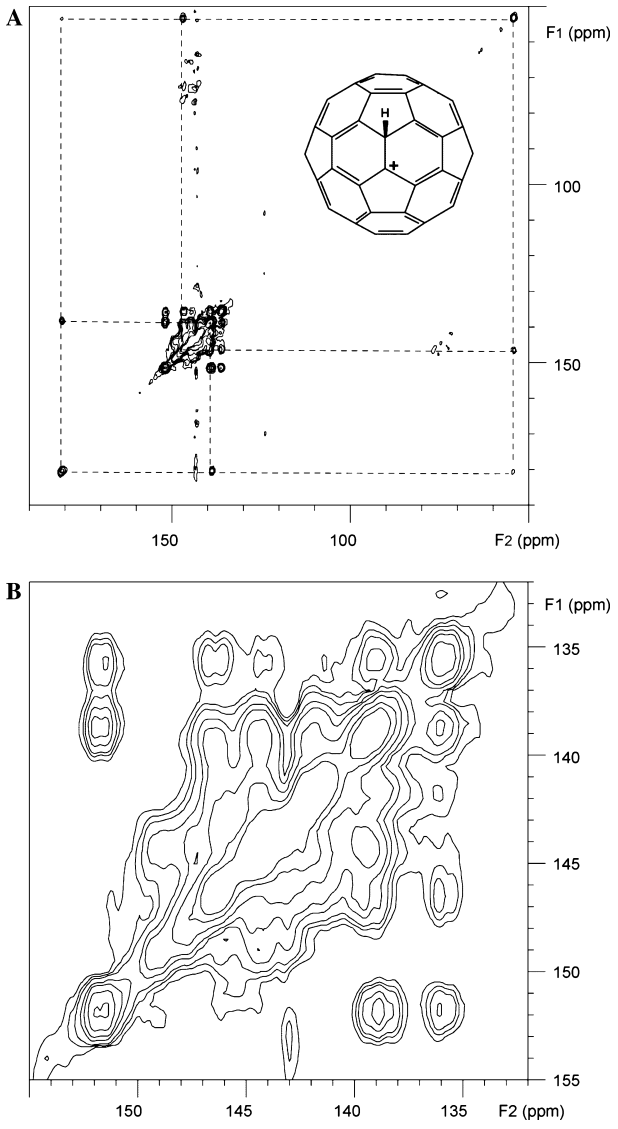

Fig. 7. The UC2QF COSY of HC_{60}^{+}. (A) The direct bond between the protonated sp^3 and the $sp^2(+)$ sites is indicated by the cross-peaks between 56 and 182 ppm. (B) An expanded view of the multitude of correlations observed in the sp^2 hybridized region. Data were acquired using the pulse sequence from Fig. 2B (with the single $\pi/2$ ^{13}C preparatory pulse) on a 9.4T Bruker DSX spectrometer (^{1}H frequency 400.13 MHz) equipped with a double resonance 4 mm MAS probe spinning at 5 kHz. Fifty kilohertz ^{13}C pulses were used throughout along with 80 kHz TPPM ^{1}H decoupling. HC_{60}^{+} was prepared from 10% ^{13}C enriched C_{60} (10% isotope abundance, randomly dispersed in the C_{60} cage) reacted with the $H(CB_{11}H_6Cl_6)$ carborane superacid as described in [35]. The 10% ^{13}C enrichment of the C_{60} allows us to consider only effective 2-spin-pair interactions, making the choice of $\tau = 1/4J_{IS} = 5$ ms most efficient.

advantages to the UC2QF COSY, particularly when the scalar couplings are small compared to the direct-observe line width.

4. Conclusions

We have introduced the UC2QF COSY, a refocused version of the popular double-quantum-filtered correlation spectroscopy experiment in liquids. The UC2QF COSY is robust for chemical shift correlation in solids by providing in-phase and doubly-absorptive line shapes. Both theory and experiment point to distinct advantages of this protocol which was originally motivated by the challenge of obtaining through-bond connectivities in dynamic solids, where global molecular motion renders dipolar-driven correlation methods ineffective, and where liquid-state methodologies proved inapplicable. In this work, we have shown that this new scalar-coupling-driven spectroscopic method can provide answers to important structural questions in the presence of dynamics, essentially independent of MAS rate, and, in favorable cases, at natural abundance ^{13}C isotope concentrations.

Acknowledgments

This work was supported by NSF Grant CHE-0349345 and Research Corporation Grant RI0461. DWE and RAO are Department of Education GAANN Fellows.

References

[1] D. Sakellariou, L. Emsley, Through-bond experiments in solids, Encyclopedia Nucl. Magn. Reson. 9 (2002) 196–211.
[2] C.A. Fyfe, Y. Feng, H. Gies, H. Grondey, G.T. Kokotailo, Natural-abundance two-dimensional solid-state ^{29}Si NMR investigations of three-dimensional lattice connectivities in zeolite structures, J. Am. Chem. Soc. 112 (1990) 3264–3270.
[3] M. Baldus, B.H. Meier, Total correlation spectroscopy in the solid state. The use of scalar couplings to determine the through-bond connectivity, J. Magn. Reson. A 121 (1996) 65–69.
[4] A. Lesage, M. Bardet, L. Emsley, Through-bond carbon–carbon connectivities in disordered solids, J. Am. Chem. Soc. 121 (1999) 10987–10993.
[5] R. Verel, J.D. van Beek, B.H. Meier, Inadequate-cr experiments in the solid state, J. Magn. Reson. 140 (1999) 300–303.
[6] J.C.C. Chan, G. Brunklaus, R sequences for the scalar-coupling mediated homonuclear correlation spectroscopy under fast magic-angle spinning, Chem. Phys. Lett. 349 (2001) 104–112.
[7] A.S.D. Heindrichs, H. Geen, C. Giordani, J.J. Titman, Improved scalar shift correlation NMR spectroscopy in solids, Chem. Phys. Lett. 335 (2001) 89–96.
[8] S.P. Brown, M. Perez-Torralba, D. Sanz, R.M. Claramunt, L. Emsley, The direct detection of a hydrogen bond in the solid state by NMR through the observation of a hydrogen-bond mediated ^{15}N–^{15}N J coupling, J. Am. Chem. Soc. 124 (2002) 1152–1153.
[9] E.H. Hardy, A. Detken, B.H. Meier, Fast-MAS total through-bond correlation spectroscopy using adiabatic pulses, J. Magn. Reson. 165 (2003) 208–218.
[10] M. Ernst, A. Detken, A. Boeckmann, B.H. Meier, NMR spectra of a microcrystalline protein at 30 kHz MAS, J. Am. Chem. Soc. 125 (2003) 15807–15810.
[11] L.J. Mueller, D.W. Elliott, K.-C. Kim, C.A. Reed, P. Boyd, Establishing through-bond connectivity in solids with NMR, structure, and dynamics in HC_{60}^{+}, J. Am. Chem. Soc. 124 (2002) 9360–9361.
[12] R.A. Olsen, J. Struppe, D.W. Elliott, R.J. Thomas, L.J. Mueller, Through-bond ^{13}C–^{13}C correlation at the natural abundance level, refining dynamic regions in the crystal structure of vitamin-D_3 with solid-state NMR, J. Am. Chem. Soc. 125 (2003) 11784–11785.
[13] L. Braunschweiler, R.R. Ernst, Coherence transfer by isotropic mixing: application to proton correlation spectroscopy, J. Magn. Reson. 53 (1983) 521–528.
[14] Y.A. Ishii, J. Ashida, T. Terao, ^{13}C–^{1}H dipolar recoupling dynamics in ^{13}C multiple-pulse solid-state NMR, Chem. Phys. Lett. 246 (1995) 439–445.
[15] A.E. Bennett, C.M. Rienstra, J.M. Griffiths, W. Zhen, J. Peter, T. Lansbury, R.G. Griffin, Homonuclear radio frequency-driven recoupling in rotating solids, J. Chem. Phys. 108 (1998) 9463–9479.
[16] R.R. Ernst, G. Bodenhausen, A. Wokaun, Principles of Nuclear Magnetic Resonance in One and Two Dimensions, Oxford University Press, Oxford, 1987.
[17] U. Piantini, O.W. Sorensen, R.R. Ernst, Multiple quantum filters for elucidating NMR coupling networks, J. Am. Chem. Soc. 104 (1982) 6800–6801.
[18] A.J. Shaka, R. Freeman, Simplification of NMR spectra by filtration through multiple-quantum coherence, J. Magn. Reson. 51 (1983) 169–173.
[19] A. Bax, R. Freeman, T.A. Frenkiel, An NMR technique for tracing out the carbon skeleton of an organic molecule, J. Am. Chem. Soc. 103 (1981) 2102–2104.
[20] W.P. Aue, E. Bartholdi, R.R. Ernst, Two-dimensional spectroscopy. Application to nuclear magnetic resonance, J. Chem. Phys. 64 (1975) 2229–2246.
[21] G. Bodenhausen, H. Kogler, R.R. Ernst, Selection of coherency-transfer pathways in NMR pulse experiments, J. Magn. Reson. 58 (1984) 370–388.
[22] M.M. Maricq, J.S. Waugh, NMR in rotating solids, J. Chem. Phys. 70 (1979) 3300–3316.
[23] O.W. Sørensen, M. Rance, R.R. Ernst, The z filters for purging phase- or multiplet-distorted spectra, J. Magn. Reson. 1969-1992 (56) (1984) 527–534.
[24] A.E. Bennett, C.M. Rienstra, M. Auger, K.V. Lakshmi, R.G. Griffin, Heteronuclear decoupling in rotating solids, J. Chem. Phys. 103 (1995) 6951–6958.
[25] B.M. Fung, A.K. Khitrin, K. Ermolaev, An improved broadband decoupling sequence for liquid crystals and solids, J. Magn. Reson. 142 (2000) 97–101.
[26] W.E. Maas, A. Bielecki, M. Ziliox, F.H. Laukien, D.G. Cory, Magnetic field gradients in solid state magic angle spinning NMR, J. Magn. Reson. 141 (1999) 29–33.
[27] A.L. Davis, J. Keeler, E.D. Laue, D. Moskau, Experiments for recording pure-absorption heteronuclear correlation spectra using pulsed field gradients, J. Magn. Reson. 98 (1992) 207–216.
[28] G.A. Morris, R. Freeman, Enhancement of nuclear magnetic resonance signals by polarization transfer, J. Am. Chem. Soc. 101 (1979) 760–762.
[29] M.R. Bendall, D.M. Doddrell, D.T. Pegg, Editing of carbon-13 NMR spectra. 1. A pulse sequence for the generation of subspectra, J. Am. Chem. Soc. 103 (1981) 4603–4605.

[30] M.H. Frey, S.J. Opella, ^{13}C spin exchange in amino acids and peptides, J. Am. Chem. Soc. 106 (1984) 4942–4945.
[31] M.G. Colombo, B.H. Meier, R.R. Ernst, Rotor-driven spin diffusion in natural-abundance ^{13}C spin systems, Chem. Phys. Lett. 146 (1988) 189.
[32] W.E. Maas, W.S. Veeman, Natural abundance ^{13}C spin diffusion enhance by magic-sngle spinning, Chem. Phys. Lett. 149 (1988) 170.
[33] R. Benn, H. Grondey, C. Brevard, A. Pagelot, The detection of connectivities of rare spin-1/2 nuclei in the solid state using natural abundance samples ^{13}C and ^{29}Si inadequate and cosy type experiments, J. Chem. Soc. Chem. Commun. (1988) 102–103.
[34] H. Kono, T. Erata, M. Takai, Determination of the through-bond carbon–carbon and carbon–proton connectivities of the native celluloses in the solid state, Macromolecules 36 (2003) 5131–5138.
[35] C.A. Reed, K.-C. Kim, R.D. Bolskar, L.J. Mueller, Taming superacids: stabilization of the fullerene cations HC_{60}^{+} and HC_{60}^{+}, Science 289 (2000) 101–104.
[36] A. Pines, M.G. Gibby, J.S. Waugh, Proton-enhanced NMR of dilute spins in solids, J. Chem. Phys. 59 (1973) 569–590.
[37] D.J. States, R.A. Haberkorn, D.J. Ruben, A two-dimensional nuclear overhauser experiment with pure absorption phase in four quadrants, J. Magn. Reson. 48 (1982) 286–292.